

NUCLEATION AND GROWTH OF HELIUM-VACANCY CLUSTERS IN IRRADIATED METALS. PART. I. A GROUP METHOD FOR AN APPROXIMATE SOLUTION OF TWO DIMENSIONAL KINETIC EQUATIONS DESCRIBING EVOLUTION OF POINT DEFECT CLUSTERS. S. I. Golubov, R. E. Stoller, S. J. Zinkle (Oak Ridge National Laboratory)*.

OBJECTIVE

The objective of the study is to develop a new grouping method for an approximate solution of two dimensional kinetic equations describing gas-assisted vacancy cluster formation in irradiated materials.

SUMMARY

Nucleation, growth and coarsening of point-defect clusters or secondary phase precipitates are of interest for many applications in solid-state physics. As an example, clusters nucleate and grow from point defects in solids through irradiation. In typical nucleation, growth and coarsening problems, a master equation (ME) is constructed that summarizes the large number of ordinary differential equations (ODE) needed to describe the evolution process. To solve the large number of ODEs in the case when it is one dimensional, e.g. clustering of vacancies and self-interstitial atoms (SIAs) under irradiation in a form of voids or dislocation loops, a grouping method was originally proposed by Kiritani [1] in 1972. In 2001 Golubov et al. [2] have shown that Kiritani's method is not adequate and developed a new grouping method. The gas-assisted nucleation of voids or bubble formation is typical of problems that require solving two-dimensional ME, which has not been subjected to any specific grouping method of the type mentioned. This work intends to fill this gap. In the present work the grouping method proposed by Golubov et al. [2] is generalized for the case of the two-dimensional one. An application of the method to the problem of helium-assisted void/bubble formation under irradiation is presented.

PROGRESS AND STATUS

1. INTRODUCTION

Precipitation of helium introduced into metals by (n,α) reactions occurring in fission and fusion reactors can lead to essential changes of the structure materials. It has been established that helium atoms assist the nucleation and growth of cavities in irradiated materials leading to swelling and change their mechanical properties. The literature contains several partial treatments of the problem at hand [2-24]. However an accurate treatment of the problem is a complicated issue thus main part of work has been done in a semi quantitative way. An exception attempt to solve the problem quantitatively has been done by Ghoniem et al. (see e.g. [22]) by using a kind of grouping method for numerical solution of a kinetic equation (KE) in a form of Fokker-Planck equation. The method developed there for two-dimensional (2-D) kinetic equation is based essentially on the same approach as it has been done in the Kiritani's one [1] in a case of one-dimensional KE, namely the evolution of clusters grouped was treated in terms of an average cluster concentration in a group. However, as it has been shown [2] for the case of one-dimensional kinetic equation, such an approach does not allowed keeping identity of the group KEs with the original ones. The main point is that the approximation of the size distribution function (SDF) within a group is failed satisfying certain conservation laws, which follow for KE and are crucially important in the problem under consideration. In the framework of the Kiritani's method the group equations has been designed by an ad hoc procedure to satisfy the conservation laws, which results in distortion of the physical mechanisms operated in the original KE. It can be shown that in the framework of the method developed in [22] the group equations do not satisfy the conservation of the total numbers of vacancies and He atoms accumulated in the clusters.

As it is shown in [2] the simplest correct grouping method in the case of one-dimensional KE may be developed when size distribution function (SDF) within a group is approximated by a linear function. It may be shown that the same approach is also valid a case when the dimensionality of KE is 2-D or higher. A grouping method based on this approach is presented in the present work.

* The work has been done in collaboration with A.M. Ovcharenko and C.H. Woo (Department of Mechanical Engineering, The Hong Kong Polytechnic University, Hong Kong)

2. MASTER EQUATION

To describe the evolution of point defect clusters or secondary phase precipitates a kinetic equation in form of the continuity equation in a phase space of a certain dimensionality defined by the vector \vec{x} is normally used

$$\frac{df(\vec{x}, t)}{dt} + \nabla J(\vec{x}, t) = 0 \quad (1)$$

where $f(\vec{x}, t)$ and $J(\vec{x}, t)$ are the number density of clusters of size \vec{x} and flux of the clusters in \vec{x} -space at time t . The ME is normally considered in two approaches. One is based on an assumption that variable size is discrete, i.e. the vector components, x_i , are described by integer values. The second one is the so called Fokker-Planck (FPE) equation where the flux $J(\vec{x}, t)$ is expanded into Taylor series and the variable \vec{x} is treated as a continuous one (see e.g. [22]). Kinetic equation based on the first approach, which is normally referred as a master equation (ME), is more general compare to that of FPE. Moreover it also allows a more detail and flexible description for the reaction kinetics of the smallest clusters. For these reasons the ME will be considered as a basic one in the present work.

In a discrete space of cluster size the variables x and m are used describe a cluster of a certain composition in the case of 2-D ME. Thus in a case of He-void cluster the variable x and m are related to a number of vacancies and He atoms in a particular cluster, respectively. A specific form of ME depends on the mechanisms, which are responsible for evolution of the clusters under irradiation (or ageing). It is commonly accepted that in many cases it is well enough to assume that the cluster of size x, m can change its size only by absorption of monomers, e.g. vacancies, self-interstitial atoms (SIAs), impurities and so on. In the case the ME can be presented as follows

$$\frac{df(x, m, t)}{dt} = [J_x(x-1, m, t) - J_x(x, m, t)] + [J_m(x, m-1, t) - J_m(x, m, t)], \begin{cases} x \geq x_{\min} \\ m \geq m_{\min} \end{cases}, \quad (2)$$

where

$$\begin{aligned} J_x(x, m, t) &= P_x(x, t)f(x, m, t) - Q_x(x+1, m, t)f(x+1, m, t), \\ J_m(x, m, t) &= P_m(x, t)f(x, m, t) - Q_m(x, m+1, t)f(x, m+1, t), \end{aligned} \quad (3)$$

and the coefficients $P_x(x, t), Q_x(x, m, t), P_m(x, t), Q_m(x, m, t)$ are the rates of capture/evaporation reactions between the monomers and clusters leading to a change in the cluster size x and m , respectively, x_{\min}, m_{\min} are minimal sizes of the clusters. For example in a case of secondary phase precipitates the values of x_{\min}, m_{\min} may be taken to be equal $x_{\min} = m_{\min} = 0$ (accept the point of $x = m = 0$). In a case of gas-vacancy clusters the choice of the parameters x_{\min}, m_{\min} is slightly different and will be discussed later.

The ME in a form of Eq. (2) is essentially a set of rate equations for clusters of each size in a size-range of practical interest. It was already pointed out (see e.g. [1]) that for practical purposes it is necessary to consider clusters containing a large number of point defects (or atoms) that makes difficulties for numerical solution even in the case 1-D kinetic equation. In the case of 2-D ME the situation is even more difficult since the total number of equations need to be solved are drastically increased compare to that of 1-D ME. Below it is shown that the grouping method developed in [2], which may be easily generalized for the case under consideration, allows solving the problem.

Note that a specific form of the coefficients $P_x(x, t), Q_x(x, m, t), P_m(x, t), Q_m(x, m, t)$ is depended on the problem of interest. An advantage of the method developed in [1] is that it may be formulated without fixing a specific form of the fluxes $J_x(x, m, t), J_m(x, m, t)$. This is the reason as to why in the following the grouping method mentioned is presented prior discussion of the mechanisms related to the gas assistant void nucleation problem. An application of the grouping method to the problem of evolution of He vacancy clusters will be presented next to illustrate use of the method.

3. BASIC EQUATIONS.

3.1. Conservation laws

Since the ME has a form of continuity equation it may be easy shown that the ME obeys certain conservation laws. As it has been shown in [2] two of them play crucial role in the case when a grouping method is used for numerical calculations. First is the conservation law for the total number of the clusters, $N(t)$. It follows from Eq. (2) that $N(t)$, which given by

$$N(t) = \sum_{x=x_{\min}}^{\infty} \sum_{m=m_{\min}}^{\infty} f(x, m, t), \quad (4)$$

is described by the following equation

$$\frac{dN(t)}{dt} = \sum_{m=m_{\min}}^{\infty} J_x(x_{\min} - 1, m, t) + \sum_{x=x_{\min}}^{\infty} J_m(x, m_{\min} - 1, t), \quad (5)$$

The second one is related to a conservation of the total number of monomers, x and m , accumulated in the clusters, $S(t)$, $M(t)$, which are given by

$$S(t) = \sum_{x=x_{\min}}^{\infty} \sum_{m=m_{\min}}^{\infty} xf(x, m, t), \quad M(t) = \sum_{x=x_{\min}}^{\infty} \sum_{m=m_{\min}}^{\infty} mf(x, m, t). \quad (6)$$

Multiplying Eq. (2) on x (or m) and summing it over x and m one can find the following equations

$$\begin{aligned} \frac{dS(t)}{dt} &= \sum_{m=m_{\min}}^{\infty} \left\{ J_x(x_{\min} - 1, m, t) + \sum_{x=x_{\min}-1}^{\infty} J_x(x, m, t) \right\} + \sum_{x=x_{\min}}^{\infty} xJ_m(x, m_{\min} - 1, t), \\ \frac{dM(t)}{dt} &= \sum_{x=x_{\min}}^{\infty} \left\{ J_m(x, m_{\min} - 1, t) + \sum_{x=x_{\min}-1}^{\infty} J_m(x, m, t) \right\} + \sum_{m=m_{\min}}^{\infty} mJ_x(x_{\min} - 1, m, t). \end{aligned} \quad (7)$$

Eq. (5) shows that, in the framework cluster evolution described by the ME, $N(t)$ changes only due to the boundary fluxes, $J_x(x_{\min} - 1, m, t)$, $J_m(x, m_{\min} - 1, t)$. In contrast to this the conservation laws described by Eqs. (7) depend on the fluxes $J_x(x, m, t)$, $J_m(x, m, t)$ in whole phase space of sizes x and m . Because of this, as it has been shown in [2] for the case of 1-D ME, the simplest approximation for the SDF inside of a group when clusters grouped are treated in terms of an average cluster concentration in a group, cannot satisfy to both conservation laws simultaneously. The situation is the same in the case of 2-D ME. Thus one may conclude that in the case under consideration the simplest grouping method has to be based on a linear approximation of SDF inside a group in respect to both variables x and m and such a method is presented in this work.

3.2. Grouping of the clusters in x, m space

Let us introduce a description of the groups in the case under consideration. Follow to [1,2] the clusters are grouped within of a group of widths $\Delta x_i = x_i - x_{i-1}$, $\Delta m_j = m_j - m_{j-1}$, which include the clusters of the sizes

$$\begin{aligned} x &= x_{i-1} + k, \quad (k = 1, \dots, \Delta x_i), \\ m &= m_{j-1} + n, \quad (n = 1, \dots, \Delta m_j), \end{aligned} \quad (8)$$

respectively, where the subscript i indicates the number of a group in x -space and the subscript j indicates the number of a group in m -space. Thus each group consists of $n_{i,j} = \Delta x_i \Delta m_j$ numbers of clusters of different sizes and is defined by the double index “ ij ”. It can be shown that the mean sizes of clusters within an ij group, $\langle x \rangle_i, \langle m \rangle_j$, are equal to

$$\begin{aligned}\langle x \rangle_i &= x_i - \frac{1}{2} (\Delta x_i - 1), \\ \langle m \rangle_j &= m_j - \frac{1}{2} (\Delta m_j - 1),\end{aligned}\tag{9}$$

respectively. Note that in a case when $\Delta x_i = 1$ or $\Delta m_j = 1$ $\langle x \rangle_i = x_i$ and $\langle m \rangle_j = m_j$, respectively.

3.3. The grouping method

Follow [2] let us approximate the SDF, $f(x, m, t)$, by a linear function within a group i, j of the type

$$f_{i,j}(x, m) = L_0^{i,j} + L_{1x}^{i,j}(x - \langle x \rangle_i) + L_m^{i,j}(m - \langle m \rangle_j).\tag{10}$$

The total number clusters in the i, j group, $N_{i,j}$, and total number of vacancies and gas atoms accumulated in the clusters, $S_{i,j}, M_{i,j}$ are given by

$$\begin{aligned}N_{i,j} &= \sum_{k=1}^{\Delta x_i} \sum_{n=1}^{\Delta m_j} f(x_{i-1} + k, m_{j-1} + n), \\ S_{i,j} &= \sum_{k=1}^{\Delta x_i} \sum_{n=1}^{\Delta m_j} (x_{i-1} + k) f(x_{i-1} + k, m_{j-1} + n), \\ M_{i,j} &= \sum_{k=1}^{\Delta x_i} \sum_{n=1}^{\Delta m_j} (m_{j-1} + n) f(x_{i-1} + k, m_{j-1} + n).\end{aligned}\tag{11}$$

Summing the ME (2) over x and m within the ij^{th} group one may find that

$$\begin{aligned}\frac{dN_{i,j}}{dt} &= \sum_{n=1}^{\Delta m_j} [J_x(x_{i-1}, m_{j-1} + n) - J_x(x_i, m_{j-1} + n)] + \\ &+ \sum_{k=1}^{\Delta x_i} [J_m(x_{i-1} + k, m_{j-1}) - J_m(x_{i-1} + k, m_j)].\end{aligned}\tag{12}$$

On the other side multiplying the Eq. (2) on x (or m) and summing it over x and m within the group one may find

$$\begin{aligned}\frac{dS_{i,j}}{dt} &= \sum_{n=1}^{\Delta m_j} \left[(x_{i-1} + 1) J_x(x_{i-1}, m_{j-1} + n) - x_i J_x(x_i, m_{j-1} + n) + \sum_{k=1}^{\Delta x_i - 1} J_x(x_{i-1} + k, m_{j-1} + n) \right] + \\ &+ \sum_{k=1}^{\Delta x_i} (x_{i-1} + k) [J_m(x_{i-1} + k, m_{j-1}) - J_m(x_{i-1} + k, m_j)],\end{aligned}\tag{13}$$

$$\begin{aligned}\frac{dM_{i,j}}{dt} &= \sum_{k=1}^{\Delta x_i} \left[(m_{j-1} + 1) J_m(x_{i-1} + k, m_{j-1}) - m_j J_m(x_i + k, m_j) + \sum_{n=1}^{\Delta m_j - 1} J_m(x_{i-1} + k, m_{j-1} + n) \right] + \\ &+ \sum_{n=1}^{\Delta m_j} (m_{j-1} + n) (J_x(x_{i-1}, m_{j-1} + n) - J_x(x_i, m_{j-1} + n)),\end{aligned}\tag{14}$$

Substituting Eq. (10) into Eq. (11) one can obtain

$$\begin{aligned} N_{i,j} &= L_0^{i,j} \Delta x_i \Delta m_j, \\ S_{i,j} &= \left(L_0^{i,j} \langle x \rangle_i + L_{1x}^{i,j} \sigma_i^2 \right) \Delta x_i \Delta m_j, \\ M_{i,j} &= \left(L_0^{i,j} \langle m \rangle_j + L_{1m}^{i,j} \sigma_j^2 \right) \Delta x_i \Delta m_j, \end{aligned} \quad (15)$$

where σ_i^2, σ_j^2 are dispersions of cluster sizes in the group, which are given by

$$\begin{aligned} \sigma_i^2 &= \frac{1}{\Delta x_i} \left[\sum_{\alpha=x_{i-1}+1}^{x_i} \alpha^2 - \frac{1}{\Delta x_i} \left(\sum_{\alpha=x_{i-1}+1}^{x_i} \alpha \right)^2 \right], \\ \sigma_j^2 &= \frac{1}{\Delta m_j} \left[\sum_{\alpha=m_{j-1}+1}^{m_j} \alpha^2 - \frac{1}{\Delta m_j} \left(\sum_{\alpha=m_{j-1}+1}^{m_j} \alpha \right)^2 \right]. \end{aligned} \quad (16)$$

It is followed from Eqs. (15) that the coefficients $L_0^{i,j}, L_{1x}^{i,j}, L_{1m}^{i,j}$ may be expressed through the moments $N_{i,j}, S_{i,j}, M_{i,j}$ as follows

$$\begin{aligned} L_0^{i,j} &= \frac{1}{\Delta x_i \Delta m_j} N_{i,j}, \\ L_{1x}^{i,j} &= \frac{1}{\Delta x_i \Delta m_j \sigma_i^2} (S_{i,j} - N_{i,j} \langle x \rangle_i), \\ L_{1m}^{i,j} &= \frac{1}{\Delta x_i \Delta m_j \sigma_j^2} (M_{i,j} - N_{i,j} \langle m \rangle_j). \end{aligned} \quad (17)$$

Differentiating Eqs. (15) over time and using Eqs. (12), (14) and (15) one can find the following equations for the coefficients $L_0^{i,j}, L_{1x}^{i,j}, L_{1m}^{i,j}$ may be written in the following form

$$\begin{aligned} \frac{dL_0^{i,j}}{dt} &= \frac{1}{\Delta x_i \Delta m_j} \left\{ \sum_{n=1}^{\Delta m_j} [J_x(x_{i-1}, m_{j-1} + n) - J_x(x_i, m_{j-1} + n)] + \right. \\ &\quad \left. \sum_{k=1}^{\Delta x_i} [J_m(x_{i-1} + k, m_{j-1}) - J_m(x_{i-1} + k, m_j)] \right\}, \end{aligned} \quad (18)$$

$$\begin{aligned} \frac{dL_{1x}^{i,j}}{dt} &= -\frac{(\Delta x_i - 1)}{2\Delta x_i \Delta m_j \sigma_i^2} \left\{ \sum_{n=1}^{\Delta m_j} [J_x(x_{i-1}, m_{j-1} + n) + J_x(x_i, m_{j-1} + n) - 2 \langle J_x \rangle_{i,n(j)}^*] \right. \\ &\quad \left. + \frac{1}{\Delta x_i - 1} \sum_{k=1}^{\Delta x_i} [(\Delta x_i + 1 - 2k)(J_m(x_{i-1} + k, m_{j-1}) - J_m(x_{i-1} + k, m_j))] \right\}, \end{aligned} \quad (19)$$

$$\begin{aligned} \frac{dL_{1m}^{i,j}}{dt} = & -\frac{(\Delta m_j - 1)}{2\Delta x_i \Delta m_j \sigma_i^2} \left\{ \sum_{k=1}^{\Delta x_i} \left[J_m(x_{i-1} + k, m_{j-1}) + J_m(x_{i-1} + k, m_j) - 2 \langle J_m \rangle_{i(k),j}^* \right] \right. \\ & \left. + \frac{1}{\Delta m_j - 1} \sum_{n=1}^{\Delta m_j} \left[(\Delta m_j + 1 - 2n) (J_x(x_{i-1}, m_{j-1} + n) - J_x(x_i, m_j + n)) \right] \right\}, \end{aligned} \quad (20)$$

where $\langle J_x \rangle_{i,n(j)}^*$ and $\langle J_m \rangle_{i(k),j}^*$ are the mean J_x flux inside ij^{th} group at a given size of m ($m = m_{j-1} + n$) and the mean J_m flux inside ij^{th} group at a given size of x ($x = x_{i-1} + k$), respectively, which are given by

$$\langle J_x \rangle_{i,n(j)}^* = \frac{1}{(\Delta x_i - 1)} \sum_{k=1}^{\Delta x_i - 1} J_x(x_{i-1} + k, m_{j-1} + n), \quad \Delta x_i > 1, \quad (21)$$

$$\langle J_m \rangle_{i(k),j}^* = \frac{1}{(\Delta m_j - 1)} \sum_{n=1}^{\Delta m_j - 1} J_m(x_{i-1} + k, m_{j-1} + n), \quad \Delta m_j > 1. \quad (22)$$

Eqs. (18) - (20) describe the evolution of the SDF within the group approximation. Thus instead of solving $n_{ij} = \Delta x_i \Delta m_j$ numbers of MEs for the group it is necessary to solve the three equations only. On the other side in the limiting cases when $\Delta x_i = 1$ or $\Delta m_j = 1$ the right hand sides of Eqs. (19) or (20) become equal to zero that results in $L_{1x}^{i,j} = 0$ or $L_{1m}^{i,j} = 0$. In the case when both widths are equal to unit, i.e. $\Delta x_i = \Delta m_j = 1$, both coefficients $L_{1x}^{i,j}$, $L_{1m}^{i,j}$ are equal to zero whereas Eq. (18) transforms to Eq. (2), that is $f(x_i, m_j) = L_0^{i,j}$. This property of the group equations is important allowing to calculate SDF using arbitrary group widths, $\Delta x_i, \Delta m_j$, including the limiting cases when $\Delta x_i = 1$ or $\Delta m_j = 1$.

Note that the group equations described by Eqs. (18) - (20) still require time consuming numerical calculations due to the summation on the right hand sides of the equations. However the equation may be simplified because the summations can be done analytically if to take an approximation that all capture/evaporation efficiencies, namely $P_x(x, m), Q_x(x, m), P_m(x, m), Q_m(x, m)$, are equal within a group (similar approximation was used in the original Kiritani's method [1]). Using this approximation and taking into account that SDF within a group linear depends on x and m (see Eq. (10)) one can find that Eqs. (18) - (20) may be finally presented in the following form

$$\frac{dL_0^{i,j}}{dt} = \frac{1}{\Delta x_i} \left[J_x(x_{i-1}, \langle m \rangle_j) - J_x(x_i, \langle m \rangle_j) \right] + \frac{1}{\Delta m_j} \left[J_m(\langle x \rangle_i, m_{j-1}) - J_m(\langle x \rangle_i, m_j) \right]. \quad (23)$$

$$\begin{aligned} \frac{dL_{1x}^{i,j}}{dt} = & -\left(\frac{\Delta x_i - 1}{2\sigma_i^2 \Delta x_i} \right) \left\{ J_x(x_{i-1}, \langle m \rangle_j) + J_x(x_i, \langle m \rangle_j) - 2J_x(\langle x_i \rangle - \frac{1}{2}, \langle m \rangle_j) \right\} \\ & + \frac{1}{\Delta m_j} \left\{ \left[J_m(\langle x \rangle_i + 1, m_{j-1}) - J_m(\langle x \rangle_i, m_{j-1}) \right] - \left[J_m(\langle x \rangle_i + 1, m_j) - J_m(\langle x \rangle_i, m_j) \right] \right\}. \end{aligned} \quad (24)$$

$$\begin{aligned} \frac{dL_{1m}^{i,j}}{dt} = & - \left(\frac{\Delta m_j - 1}{2\sigma_j^2 \Delta m_j} \right) \left\{ J_m(\langle x \rangle_i, m_{j-1}) + J_m(\langle x \rangle_i, m_j) - 2J_m(\langle x \rangle_i, \langle m \rangle_j - \frac{1}{2}) \right\} \\ & + \frac{1}{\Delta x_i} \left\{ \left[J_x(x_{i-1}, \langle m \rangle_j + 1) - J_x(x_{i-1}, \langle m \rangle_j) \right] - \left[J_x(x_i, \langle m \rangle_j + 1) - J_x(x_i, \langle m \rangle_j) \right] \right\}. \end{aligned} \quad (25)$$

Eqs. (23) - (25) describe the evolution of the SDF within the group approximation. Note that last two equations are highly symmetrical, e.g. one may obtain Eq. (25) from Eq. (24) by using a simple permutation of fluxes J_x, J_m with corresponding change of the variables x to m and m to x and the multiplier $\frac{\Delta x_i - 1}{2\sigma_i^2 \Delta x_i}$ to $\frac{\Delta m_j - 1}{2\sigma_j^2 \Delta m_j}$.

3.4. The grouping method in the cases of 1-D and 3-D ME

In the case of 1-D ME, i.e. when $f(x, m) = f(x)$, Eqs. (23) - (25) are transformed to the equations (37) and (38) derived in [2] for the case of 1-D ME. Actually in this case the flux J_m and coefficient $L_{1m}^{i,j}$ are equal to zero, $J_m = 0, L_{1m}^{i,j} = 0$, that transforms Eqs. (23), (24) in

$$\begin{aligned} \frac{dL_0^{i,j}}{dt} &= \frac{1}{\Delta x_i} [J_x(x_{i-1}) - J_x(x_i)], \\ \frac{dL_{1x}^{i,j}}{dt} &= - \left(\frac{\Delta x_i - 1}{2\sigma_i^2 \Delta x_i} \right) \left\{ J_x(x_{i-1}) + J_x(x_i) - 2J_x(\langle x_i \rangle - \frac{1}{2}) \right\}. \end{aligned} \quad (26)$$

It is easy to show that Eqs. (26) coincide with the equations (37) and (38) in [2] taking into account that the mean flux $\langle J \rangle_i^*$ in [2] (see Eq. (38)) is equal to $J_x(\langle x_i \rangle - \frac{1}{2})$ in the case when the capture/evaporation efficiencies, namely $P_x(x, m)/Q_x(x, m)$, are taken to be equal within a group. Note, as it already has been pointed out in [25], the multiplier $-1/\Delta x_i$ in the right hand side of Eq. (38) in [2] was lost.

On the other side it is worthy to emphasize that the symmetry of Eqs. (23) - (25) allows one easily to generalize the grouping method on a case when dimensionality of the ME is higher than two. For example in the case of 3-D ME, i.e. when the SDF depends on three variables ($f(x, m, n)$) the approximation of SDF within a group (see Eq. (10)) is given by

$$f_{i,j,k}(x, m) = L_0^{i,j,k} + L_{1x}^{i,j,k}(x - \langle x \rangle_i) + L_{1m}^{i,j,k}(m - \langle m \rangle_j) + L_{1n}^{i,j,k}(n - \langle n \rangle_k). \quad (27)$$

In the case one can easily find that Eq. (23) takes a form

$$\begin{aligned} \frac{dL_0^{i,j,k}}{dt} &= \frac{1}{\Delta x_i} [J_x(x_{i-1}, \langle m \rangle_j, \langle n \rangle_k) - J_x(x_i, \langle m \rangle_j, \langle n \rangle_k)] \\ &+ \frac{1}{\Delta m_j} [J_m(\langle x \rangle_i, m_{j-1}, \langle n \rangle_k) - J_m(\langle x \rangle_i, m_j, \langle n \rangle_k)] \\ &+ \frac{1}{\Delta n_k} [J_n(\langle x \rangle_i, \langle m \rangle_j, n_{k-1}) - J_n(\langle x \rangle_i, \langle m \rangle_j, n_k)]. \end{aligned} \quad (28)$$

where $J_l(x, m, n)$ is the flux of the clusters in l direction ($l = x, m, n$). The same way one can generalize Eqs. (24) and (25). For example one can find that Eq. (24) takes a form

$$\begin{aligned}
\frac{dL_{1x}^{i,j,k}}{dt} = & - \left(\frac{\Delta x_i - 1}{2\sigma_i^2 \Delta x_i} \right) \left\{ J_x(x_{i-1}, \langle m \rangle_j, \langle n \rangle_k) + J_x(x_i, \langle m \rangle_j, \langle n \rangle_k) \right. \\
& \left. - 2J_x(\langle x \rangle_i - \frac{1}{2}, \langle m \rangle_j, \langle n \rangle_k) \right\} \\
& + \frac{1}{\Delta m_j} \left\{ \left[J_m(\langle x \rangle_i + 1, m_{j-1}, \langle n \rangle_k) - J_m(\langle x \rangle_i, m_{j-1}, \langle n \rangle_k) \right] \right. \\
& \left. - \left[J_m(\langle x \rangle_i + 1, m_j, \langle n \rangle_k) - J_m(\langle x \rangle_i, m_j, \langle n \rangle_k) \right] \right\} \\
& + \frac{1}{\Delta n_k} \left\{ \left[J_n(\langle x \rangle_i + 1, \langle m \rangle_j, n_{k-1}) - J_n(\langle x \rangle_i, \langle m \rangle_j, n_{k-1}) \right] \right. \\
& \left. - \left[J_n(\langle x \rangle_i + 1, \langle m \rangle_j, n_k) - J_n(\langle x \rangle_i, \langle m \rangle_j, n_k) \right] \right\}.
\end{aligned} \tag{29}$$

The equations for the coefficients $L_{1m}^{i,j}, L_{1n}^{i,j}$ can be easily obtained from Eq. (29) by permutation of fluxes J_x, J_m, J_n with corresponding change of the variables x, m and n and the multiplier $\frac{\Delta x_i - 1}{2\sigma_i^2 \Delta x_i}$ to $\frac{\Delta m_j - 1}{2\sigma_j^2 \Delta m_j}$ or $\frac{\Delta n_k - 1}{2\sigma_k^2 \Delta n_k}$, respectively, on the right hand side of the equation. The grouping equations in the case when dimensionality of the ME is higher than three may be obtained by the same way.

4. MODEL DESCRIPTION

In order to use the grouping method one need to set up a model of interest. As can be seen from the ME and Eqs. (23) - (25) a model is fully determined by a choice of the fluxes $J_x(x, m, t), J_m(x, m, t)$. In this paper He-assisted vacancy clustering in irradiated metals is considered only. For the sake of simplicity in the following the process is considered taking into account single mechanism of He transport only, namely via migration of He atoms in a form of the interstitials.

4.1. Flux $J_x(x, m, t)$

In the first Eq. (3) $P_x(x, t)$ and $Q_x(x, m, t)$ are the rate of a vacancy absorption and the sum of corresponding rates of SIAs absorption (in the case of irradiation) and vacancy emission from the clusters of size x containing m He atoms. In the following the SIAs are considered having two configurations, namely the dumbbell configuration, which is 3-D diffusing defect, and crowdion configuration, which is 1-D diffusing defect. Last configuration is chosen to represent the SIA clusters, which are normally generated in irradiated metals under cascade damage conditions. Such a simplification is taken due two reasons: (a) the 1-D reaction kinetics is not very sensitive to the size of the SIA clusters, (b) in the case of crowdions the ME still keeps the form of Eq. (2). In the case when concentrations of 3-D diffusing point defects, $C_v(t), C_i(t)$, and 1-D diffusing crowdions, $C_g(t)$, are measured in atomic fractions the rates $P_x(x, t)$ and $Q_x(x, m, t)$ may be written as follows [26]

$$\begin{aligned}
P_x(x) &= wx^{1/2} D_v C_v(t), \\
Q_x(x, m) &= wx^{1/2} \left[D_i C_i + D_v \exp(-E_v^b(x, m)/kT) \right] + Q_x^g(x, t) = Q_x^i(x, m) + Q_x^v(x, m) + Q_x^g(x, t), \tag{30} \\
Q_g(x, t) &= 2\Lambda D_g C_g \left(\frac{3\sqrt{\pi}\Omega}{4} \right)^{2/3} x^{2/3}, \quad \Lambda = \sqrt{\frac{k_g^2}{2}},
\end{aligned}$$

where $w = (48\pi^2/\Omega^2)^{1/3}$ (Ω is the atomic volume), D_v, D_i and D_g are the diffusion coefficients of 3-D diffusing vacancies and SIAs and 1-D diffusing crowdions, respectively; $E_v^b(x, m)$ is a binding energy of vacancy with a cluster of size x containing m gas atoms, k_B is the Boltzmann constant, T is absolute temperature. The value k_g^2 in the last equation is the total sink strength for the crowdions, which is given by [26]

$$k_g^2 = 2 \left(\frac{\pi\rho d_{abs}}{4} + \sqrt{\frac{2}{l(2R_g - l)}} + \sigma_v N_v + \sigma_{vc} N_{vc} + \sigma_{ic} N_{ic} \right)^2, \quad (31)$$

where $\sigma_v = \pi R_v^2$, R_v and N_v are the void radius and density, d_{abs} is the capture diameter of dislocations for the absorption of the SIA clusters, σ_{vc}, σ_{ic} and N_{vc}, N_{ic} are the mean cross-sections of the sessile vacancy and SIA clusters and number densities of these clusters, respectively; R_g, l are the grain radius and distance from the grain boundary, respectively. The cross section of voids, $\sigma_v N_v$, can be easily calculated using SDF

$$\sigma_v N_v = \sum_{x=2}^{\infty} \sum_{m=0}^{\infty} Q_g(x, t) f(x, m, t) + Q_g(1, t) \sum_{m=1}^{m_0} f(1, m, t). \quad (32)$$

Binding energy

The binding energy of vacancies with the clusters, $E_v^b(x, m)$, is a key ‘‘parameter’’ controlling nucleation of the clusters. Assuming that the volume of a cluster, V , does not depend on the parameter m , i.e. it obeys the equation $V = x\Omega$ (Ω is atomic volume), and taking into account that the pressure produced by m He atoms in a spherical cluster containing x vacancies, $p(x, m)$, may be presented as $p(x, m) = (k_B T / \Omega)(m/x)Z(m/x, T)$, where $Z(T, m/x)$ is so called compressibility factor, one can find that the $E_v^b(x, m)$ may be written as

$$E_v^b(x, m) = E_v^f - \frac{\alpha}{x^{1/3}} + \left(\frac{m}{x} \right) Z \left(\frac{m}{x}, T \right) k_B T, \quad (33)$$

where E_v^f is the vacancy formation energy, $\alpha = 2\gamma(4\pi\Omega^2/3)^{1/3}$ and γ is the free surface energy. The function $Z(T, m/x)$ depends on an approach used to calculate the equation of state (EOS) of He. Several approximations to the EOS have been proposed so far. In the following two equations of state are tested. The first one is so called hard sphere EOS [27], which results in the function $Z_{hs}(m/x, T)$ given by

$$Z(T, m/x)_{hs} = \frac{(1 + y + y^2 - y^3)}{(1 - y)^3}, \quad (34)$$

$$y = \left(\frac{\pi d^3}{6\Omega} \right) \frac{m}{x},$$

where d is the hard sphere diameter of He atom. The diameter d is a temperature dependent function, which is given by $d = 0.3135 \cdot [0.8542 - 0.03996 \cdot \ln(T/9.16)]$ nm.

The second EOS was derived by Manzke et al [28] by using Beck’s potential and interpolation between a quasi-harmonic approximation with anharmonic corrections for solid fcc He, which results in the function $Z_m(m/x, T)$,

which after a simplification (combining the first and last terms in Eq. (3) in [28] and taking into account that the multiplier $Z'_m V'_m$ in the last one is equal to $Z'_m V'_m = -50$) can be presented as

$$Z_m(T, m/x) = (1 - \rho) \left(1 + \rho - 52\rho^2 \right) + \frac{b}{V_m} \rho (1 - \rho)^2 + Z_m \rho^2 (3 - 2\rho), \quad (35)$$

where

$$\begin{aligned} \rho &= \left(\frac{V_m}{\Omega} \right) \frac{m}{x}, \\ V_m &= 56 T^{-1/4} \exp(-0.145 T^{1/4}), \\ Z_m &= 0.1225 V_m T^{0.555}, \\ b &= 170 T^{-1/3} - 1750 T^{-1}. \end{aligned} \quad (36)$$

In Eqs. (36) V_m is the He atomic volume of the melt measured in cubic angstroms. Note that Eqs. (36) are written here assuming that the volume of the cluster containing x vacancies, V , is equal to $V = x\Omega$.

4.2. Flux $J_m(x, m, t)$

In the second Eq. (3) $P_m(x, m, t)$ is the rate of a He atom absorption by a cluster of size x and $Q_m(x, m, t)$ is a rate of resolution of He atoms from the clusters of size x containing m He atoms. The rate $P_m(x, m, t)$ may be calculated the same way as used for point defects whereas an equation for the rate $Q_m(x, m, t)$ depend on a mechanism responsible for resolution of He atoms from the clusters. In a case of so called radiation resolution mechanism (see e.g. [6]) the rate $Q_m(x, m, t)$ is linear dependent on the number of He atoms in a cluster. Taking into account the radiation resolution mechanism only $P_m(x, m, t)$ and $Q_m(x, m, t)$ may be written as

$$\begin{aligned} P_m(x) &= wx^{1/3} D_{He} C_{He}, \\ Q_m(x, m) &= Am, \end{aligned} \quad (37)$$

where $C_{He}(t)$ and D_{He} are the concentration and diffusion coefficient of He atoms in the interstitial position and A is a parameter characterizing intensity of the radiation resolution mechanism.

Equations (30) - (37) fully determine the model under consideration. All capture/evaporation rates need to be used to calculate the fluxes $J_x(x, m, t)$, $J_m(x, m, t)$ can be calculated using these equations together with the equations for the concentrations of the mobile defects, which are presented in the next section.

4.3. Equations for the concentrations of mobile defects

As it has been already shown in [26] the rate equations for point defect concentrations of mobile defects, $C_v(t)$, $C_i(t)$, $C_g(t)$, are given by

$$\begin{aligned} \frac{dC_v}{dt} &= \left\{ G_v + Q_m(1)f(1,1,t) + Q_x(2,0)f(2,0,t) + \sum_{x=2}^{\infty} \sum_{m=0}^{\infty} Q_x^v(x+1,m)f(x+1,m,t) + D_v C_{v0} Z_v \rho_d \right\} \\ &- \left[\mu_R D_i C_i C_v + \mu_R^{He} D_{He} C_{He} C_v + D_v C_v Z_v \rho_d + P_x(1)f(1,0,t) + \sum_{x=1}^{\infty} \sum_{m=0}^{\infty} P_x(x)f(x,m,t) \right], \end{aligned} \quad (38)$$

$$\frac{dC_i}{dt} = G_i - \mu_R D_i C_i C_v - D_i C_i Z_i \rho_d - \sum_{x=2}^{\infty} \sum_{m=0}^{m_{\max}} Q_x^i(x) f(x, m, t) - Q_x^i(1) \sum_{m=1}^{m=m_0} f(1, m). \quad (39)$$

$$\frac{dC_g(t)}{dt} = G_g(t) - D_g C_g(t) k_g^2(t), \quad (40)$$

where G_v, G_i, G_g are the generation rates of vacancies, SIAs (in dumbbell and crowdion configurations) and He atoms, respectively, μ_R is the coefficients describing reactions between SIA and vacancy, Z_v, Z_i are the capture efficiencies of dislocations for vacancies and SIAs, respectively, ρ is the dislocation density, C_{v0} is the thermal equilibrium vacancy concentration, m_0 is the maximum number of He atoms in the clusters of the smallest size, $f(1, m)$. The generation rates vacancies and SIAs are given by

$$\begin{aligned} G_v &= G_{NRT} (1 - \varepsilon_r), \\ G_i &= G_{NRT} (1 - \varepsilon_r) (1 - \varepsilon_i^g), \\ G_g &= G_{NRT} (1 - \varepsilon_r) \varepsilon_i^g, \end{aligned} \quad (41)$$

where G_{NRT} is the generation rate calculated using NRT model, ε_r is a fraction of point defects recombined during cooling phase of cascades, ε_i^g is a fraction SIAs generated in a the form of crowdions. Note that vacancy clustering in a form of dislocation loops or stacking fault tetrahedra, which also takes place during cooling phase of cascades, is not considered in this work.

Equation for the concentration of He atoms in the interstitial position may be written in the same manner

$$\begin{aligned} \frac{dC_{He}}{dt} &= \left\{ G_{He} + \sum_{x=2}^{\infty} \sum_{m=1}^{m_{\max}} Q_m(m) f(x, m, t) + \sum_{m=1}^{m=m_0} [Q_m(m) + m Q_x^i(1)] f(1, m) \right\} \\ &- \left[\mu_R D_{He} C_v C_{He} + D_{He} C_{He} Z_{He} \rho_d + \sum_{x=2}^{\infty} \sum_{m=0}^{m_{\max}-1} P_m(x) f(x, m, t) + P_m(1) \sum_{m=1}^{m=m_0-1} f(1, m) \right], \end{aligned} \quad (42)$$

where G_{He} is the generation rate of He atoms, μ_R^{He} is the coefficients describing reaction between He atom and vacancy, Z_{He} is the capture efficiencies of dislocations for He atoms.

The terms in the figure brackets on the right hand side of Eqs. (38) and (42) describe the generation of vacancies and interstitial He atoms via irradiation and due to reactions of the smallest clusters with the mobile defects. Note that the capture/evaporation terms on the right hand side Eq. (42) for the clusters of the smallest size are written separately to show explicitly limitation in increase of number of He atoms in the clusters (see last term in the square brackets) and the replacement reaction caused by interaction o the clusters with SIAs (see last term in the figure brackets).

4.4. Initial and boundary conditions

The initial conditions for the mobile defects and boundary conditions for the SDF are taken to have the following form

$$\begin{aligned} C_v(t)|_{t=0} &= C_{v0}, \quad C_i(t=0)|_{t=0} = C_g(t=0)|_{t=0} = C_{He}(t)|_{t=0} = 0, \\ f(x, m, t)|_{t=0} &= C_{v0} \delta(x-1) \delta(m) + C_{He}^{lm} \delta(x-1) \delta(m-1), \quad (x \geq 1), \\ f(x=1, 0, t) &= C_v(t), \quad f(x=\infty, m, t) = 0, \end{aligned} \quad (43)$$

where C_{He}^{lm} is the concentration of He pre implanted in a metal before irradiation. Thus in the following it is assumed that all pre implanted He atoms take the substitution configuration, i.e. takes a form of the (1,1) cluster. Note that such an assumption is a kind of simplification since during an implantation a kind of SDF of He-vacancy clusters has to be formed. However the clusters produced normally via pre implantation are very small and practically this SDF is not measured. Thus for the sake of simplicity it looks reasonable to use the initial condition given by the third Eq. (43). Note that the calculations of type presented in this work can be easily carried out taking into account an arbitrary initial SDF. Moreover in principle a SDF produced during pre implantation can be calculated by using the same type of calculations.

5. RESULTS AND DISCUSSION

In the calculations a nickel type of metal is considered under irradiation with the parameters close to that taking place in fast breeder reactors. The set of main parameters used in the calculations is given in the Table 1.

Table 1. Parameters used in the calculation.

Temperature, T	473-973K
NRT displacement rate, G_{NRT}	10^{-6} dpa/s
Recombination fraction, ε_v	0.75
Fraction of crowdions, ε_i^g	0; 0.1
Effective displacement rates, $G_v = G_i + G_g = G_{NRT}(1 - \varepsilon_v)$	$2.5 \cdot 10^{-7}$ dpa/s
Helium generation rate, G_{He}	(1 -100) ppm/dpa
Recombination coefficients, $\mu_R = \mu_R^{He}$	$5.0 \cdot 10^{+20} \text{ m}^{-2}$
Atomic volume, Ω	$1.205 \cdot 10^{-29} \text{ m}^{-3}$
Vacancy diffusion coefficient, D_v	
pre-exponent coefficient	$1.0 \cdot 10^{-06} \text{ m}^2/\text{s}$
migration energy	1.10 eV
SIA diffusion coefficient, D_i	
pre-exponent coefficient	$1.0 \cdot 10^{-08} \text{ m}^2/\text{s}$
migration energy	0.15 eV
He diffusion coefficient, D_{He}	
pre-exponent coefficient	$1.0 \cdot 10^{-08} \text{ m}^2/\text{s}$
migration energy	0.15 eV
Dislocation density, ρ_d	10^{13} m^{-2}
Free surface energy, γ	$(1 - 2) \cdot 10^3 \text{ mJ}/\text{m}^2$
Dislocation capture efficiency for vacancies, Z_v	1.00
Dislocation capture efficiency for SIAs, Z_i	1.25
Dislocation capture efficiency for He atoms, Z_{He}	0
Rate of radiation resolution, A	0

5.1. Homogeneous nucleation

In the case of absent of gas impurities the nucleation of 3-D vacancy clusters occurs via so called homogeneous mechanism, which has been developed in great details (see e.g. [29]-[31]). Gas-assistant mechanism of the nucleation operate simultaneously with the previous one thus in order to emphasize the He effect on the nucleation and growth of the clusters it is useful to present a brief description of the process in the limiting case when there are not He atoms in irradiated material, which is described by the equations given above at $C_{He}^{lm} = 0$, $G_{He} = 0$.

As can be seen from Eq. (33) the surface energy γ is the main parameter at $m=0$, which controls the binding energy $E_b(x, m=0)$. The value of γ in Ni is somewhat close to $2000 \text{ mJ}/\text{m}^2$ and slightly depends on temperature [31] but in some cases (see e.g. [31]) it has been taken to be essentially lower (e.g. $1000 \text{ mJ}/\text{m}^2$ [7]). To illustrate an

influence of the parameter γ on the nucleation of the clusters in the following the value γ is chosen to be in a range of 1000 -2000 mJ/m². The corresponding binding energy in the case $m=0$ is presented in Fig. 1. As can be seen from the plot the binding energy $E_b(x, m=0)$ essentially decreases with increase of γ that, in its turn, has to result in decrease of nucleation rate of the clusters. The calculated results illustrating such dependence are presented in Figs. 2 -6.

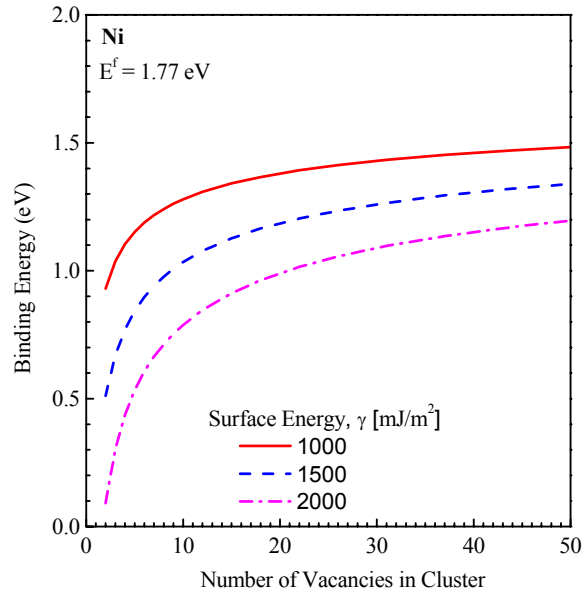


Fig. 1. The binding energy of a vacancy with voids at different values of the free surface energy.

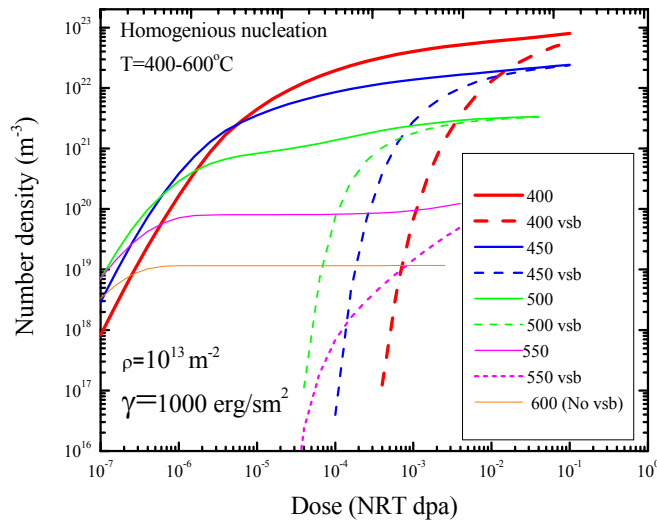


Fig. 2. Dose dependence of total number density of void under irradiation in the temperature range of 400-600°C in the case of homogeneous nucleation. The solid lines represent the total density of all vacancy clusters whereas the non-solid lines represent the total density of so called "visible" clusters, which are defined here as the cluster with the sizes of $x > 20$. Note that there are no visible clusters at 600°C.

The dose dependence of number density of void nucleated under irradiation in the temperature range of 400-600°C and $\gamma=1000$ (the value γ here and in the following is measured in mJ/m^2) is presented in Fig. 2. The solid lines represent the total density of vacancy clusters whereas the non-solid lines represent the total density of visible clusters. Note that there are no visible clusters at 600°C that means the nucleation rate is equal to zero. This can be clearly seen from Fig. 3 and 4 where the dose dependence of swelling corresponding to the irradiation conditions presented on Fig. 2 and the size distribution functions calculated at 10^{-2} dpa are presented. As can be seen from Fig. 3 vacancy accumulation in the clusters is delay already at $T=550^\circ\text{C}$ and completely saturated at a very low level at $T=600^\circ\text{C}$. The temperature dependence of the visible density of the clusters, which represent the terminal cluster density nucleated during irradiation, is presented in Fig. 5.

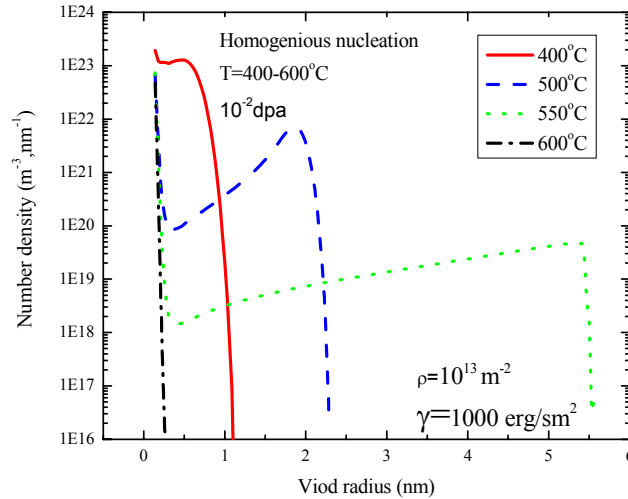


Fig. 3. Size distribution functions of the clusters at irradiation dose of 10^{-2} dpa in the case of homogeneous nucleation.

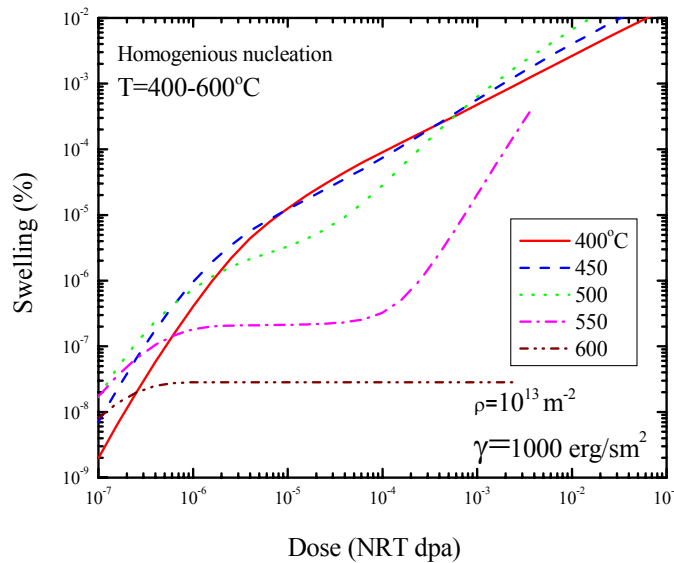


Fig. 4. Dose dependence of swelling in the case of homogeneous nucleation. Note that swelling is saturated at 600°C.

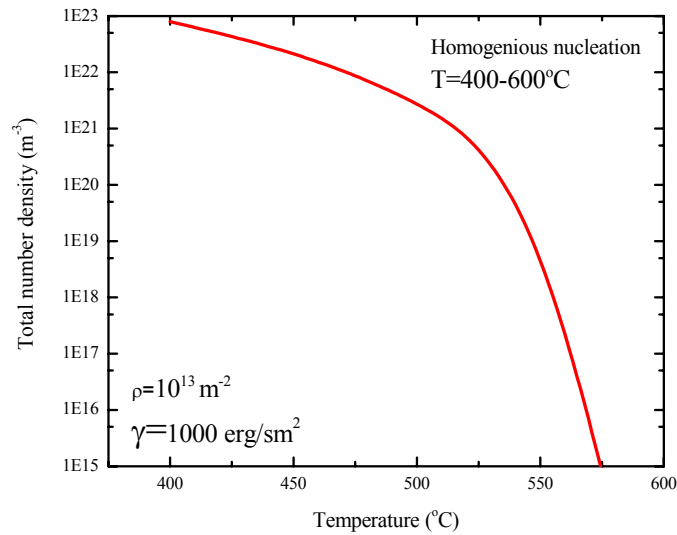


Fig. 5. Temperature dependence of the terminal cluster density in the case of homogeneous nucleation.

The dose dependence of the number density of the clusters calculated at $\gamma=1500$ and 2000 are presented in Fig. 6 and 7. As can be seen from the Fig. 2, 6 and 7 the increase of γ shifts drastically the temperature interval where the homogeneous nucleation mechanism is effective towards to low temperatures. It is shown below that the situation is quite different when the helium generation is taken into account.

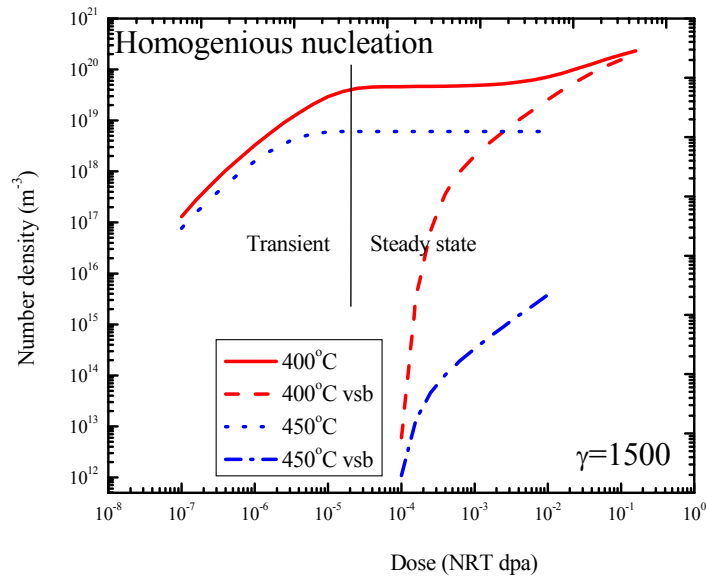


Fig. 6. Dose dependence of the cluster density in the range of 400° - 450°C at $\gamma = 1500$ in the case of homogeneous cluster nucleation. Note that the vertical line marks the beginning of the steady state for point defect concentrations.

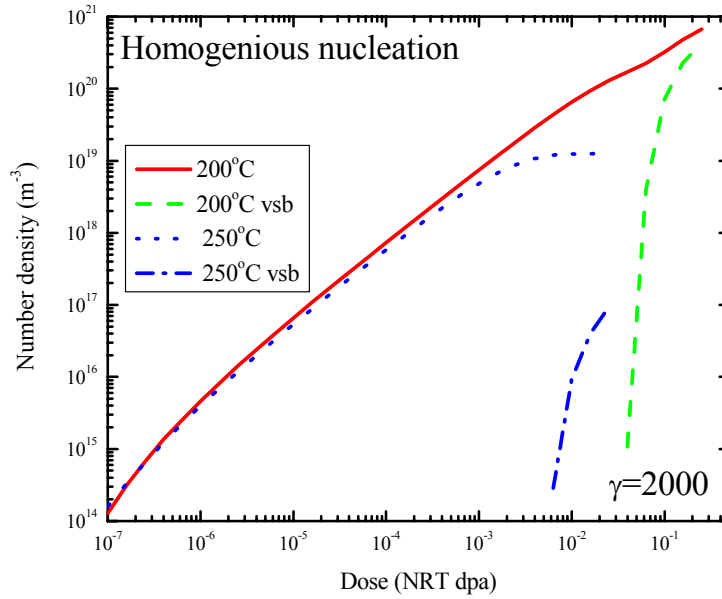


Fig. 7. Dose dependence of the cluster density in the range of 200°-250°C at $\gamma = 2000$ in the case of homogeneous cluster nucleation..

5.2. Evolution of helium-vacancy clusters

Binding energy

As can be seen from Eq. (33) the binding energy of vacancies with a cluster s increases in the case when He atoms filled in the cluster. The binding energy calculated by using EOS described by Eq. (35) as a function of x and m at different temperatures and values of the surface energy, γ , is shown in Fig.8a -8c. In Figs. 8a and 8b the binding energy is presented for the lowest value of the surface energy of $\gamma=1000$ at 300° and 600°C, respectively. It can be seen (see the projections on x, m plane) that the binding energy is slightly increased with increasing temperature that is related to an increase of the pressure produced by the gas atoms inside of the clusters. On the other side as can be seen from Figs. 8b and 8c the binding energy is essentially decreases with increase of the surface energy from 1000 to 2000. Note that for the sake simplicity the value of the binding energy for the clusters presented in Figs. 8 are taken to be equal to E_v^f when it is larger than the formation energy of vacancy, E_v^f , since there are no difference between those clusters which obey the inequality $E_b(x, m) \geq E_v^f$ in respect of their ability to evaporate vacancies (all of them are practically thermally stable at temperatures of interest). Note that the function $E_b(x, m)$ calculated by using EOS (34) is very close to that presented in Figs. 8.

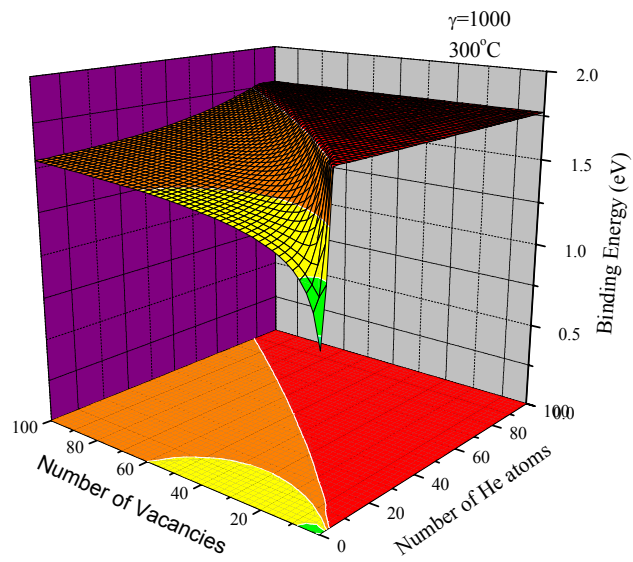


Fig. 8a. The binding energy of a vacancy with He-vacancy clusters at $T=300^{\circ}\text{C}$ and $\gamma=1000$.

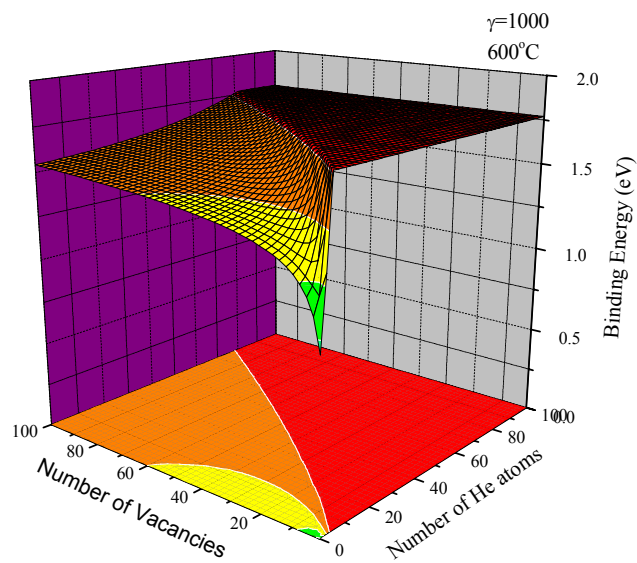


Fig. 8b. The binding energy of a vacancy with He-vacancy clusters at $T=600^{\circ}\text{C}$ and $\gamma=1000$.

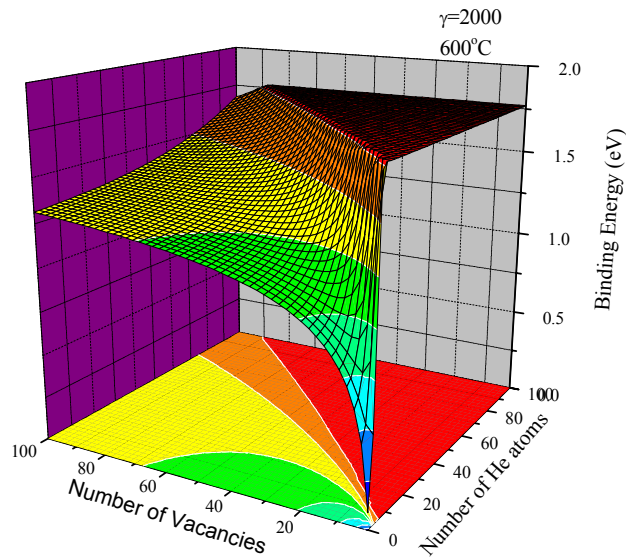


Fig. 8c. The binding energy of a vacancy with He-vacancy clusters at $T=600^{\circ}\text{C}$ and $\gamma=2000$.

Cluster evolution under irradiation

The cluster evolution, which takes place under irradiation, depends on material parameters on one side and irradiation conditions on another side. Full scale study of the process is a complicated problem and it is not the issue for the present work. As it already has been emphasized the main objective here is to present some preliminary results of He-vacancy cluster evolution obtained by using the grouping method developed. For the sake of simplicity in the following the results calculated in the framework of the standard rate approach for a particular case, when He atoms are generated concurrently with point defects and $C_{He}^{lm} = 0$, are presented only.

It has been shown above the homogeneous mechanism void nucleation is failed at high temperatures. In the case of $\gamma=1000$ (see Fig. 2) the homogeneous nucleation does not occur already at $T=600^{\circ}\text{C}$. Thus one may conclude that the cluster nucleation at $T=600^{\circ}\text{C}$ in the case when generation of He atoms takes place occurs due to formation of He-vacancy clusters. Due to the reason this temperature is chosen for the calculations and the results obtained are presented below.

Figure 9 shows the dose dependence of the total number density ($x \geq 1$ excluding vacancy concentration) and density of visible clusters ($x > 20$) of the clusters, N_{vis}^{lm} , obtained by the calculations for three different He generation rates, namely 1, 10 and 100 ppm/dpa. For a comparison the total number density calculated in the case of homogeneous nucleation is also presented. As can be seen nucleation of the clusters occurs practically in the pure homogeneous way at low doses, when number of He atoms generated is small. However already at a dose of order of 10^6 dpa the gas atoms start to accelerate the cluster formation providing finally nucleation of the visible clusters, which are stable and grow at the irradiation conditions considered. Stability of the clusters can be clearly seen on Fig. 10 where the dose dependence of swelling is presented. Thus one can conclude that generation of gas atoms leads to increase of the upper temperature limit for the nucleation that is shown in Fig. 11.

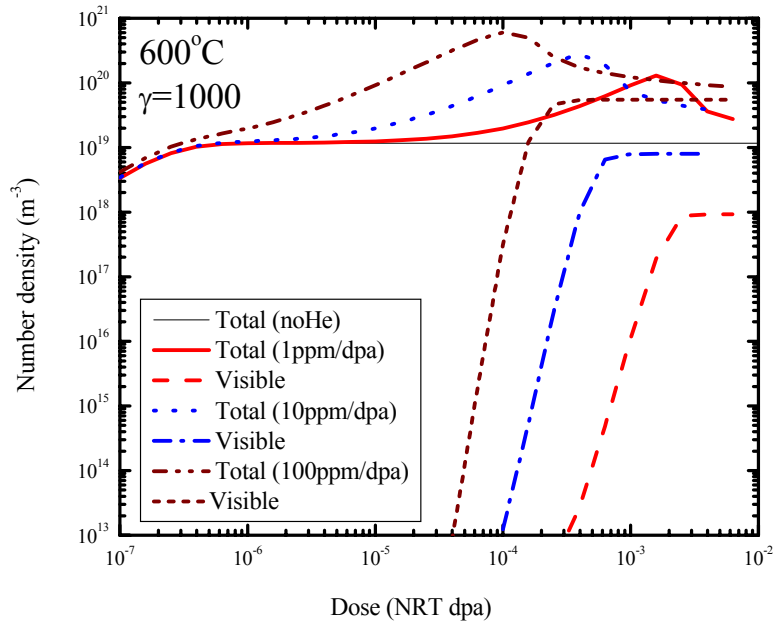


Fig. 9. Dose dependence of the cluster density at different He generation rates under irradiation at 600°C. Note that the curve drawn by the thin line corresponds to the total cluster density in the case of homogeneous nucleation.

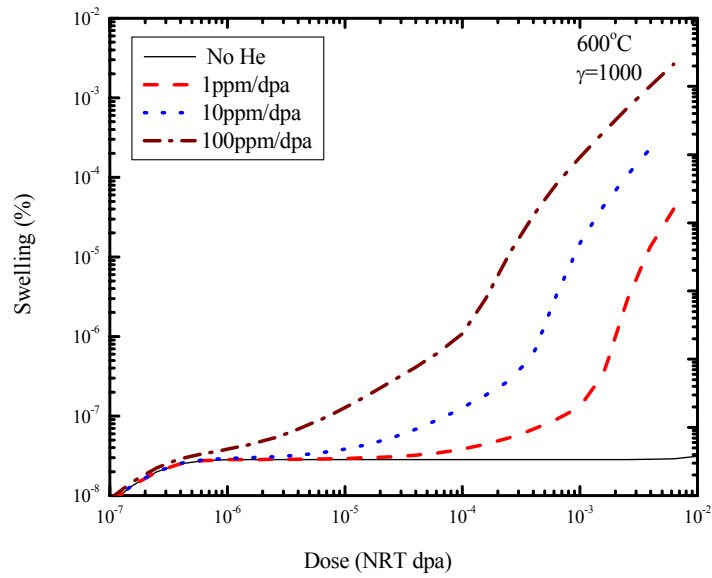


Fig. 10. Dose dependence of swelling at different He generation rates under irradiation at 600°C. Note that the curve drawn by the thin line corresponds to the swelling in the case of homogeneous nucleation.

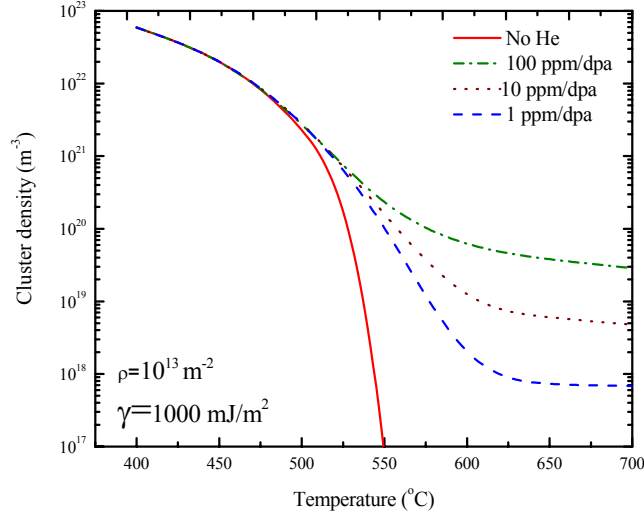


Fig. 11. Temperature dependence of the cluster density under irradiation in the temperature range of 400–600°C. The solid curve corresponds to the homogeneous nucleation, the other curves correspond to the cases of the He generation rates $G_{He} = 1, 10$ and 100 ppm/dpa.

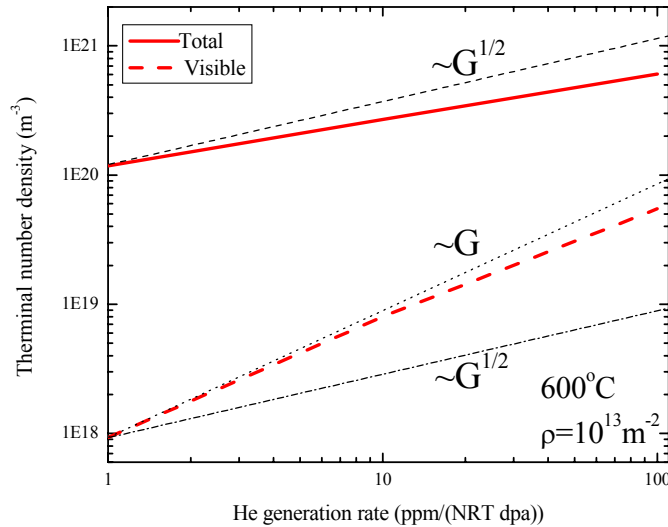


Fig. 12. Dependence of the cluster density on the He generation rate under irradiation at 600°C. Note that the solid line corresponds to a maximum of the total number density of the clusters.

Figure 12 shows the dependence of the cluster density on the He generation rate, where the thick solid and dashed lines correspond to a maximal value of the total number density and number density of the visible clusters, respectively (see Fig. 9). As can be seen the maximal magnitude of the total number density increases with the generation rate increase with increasing the generation rate G_{He} . However the increase is rather weak (less than that of the square root (see the upper thin line)). In contrast the number density of visible clusters increases much strongly being very close to that described by the linear one (the corresponding linear and square root dependences are also shown on the plot). Thus one can conclude that the dependence $N_{vis}(G_{He})$ that agrees quite well with that predicted by Trinkaus [12, 13].

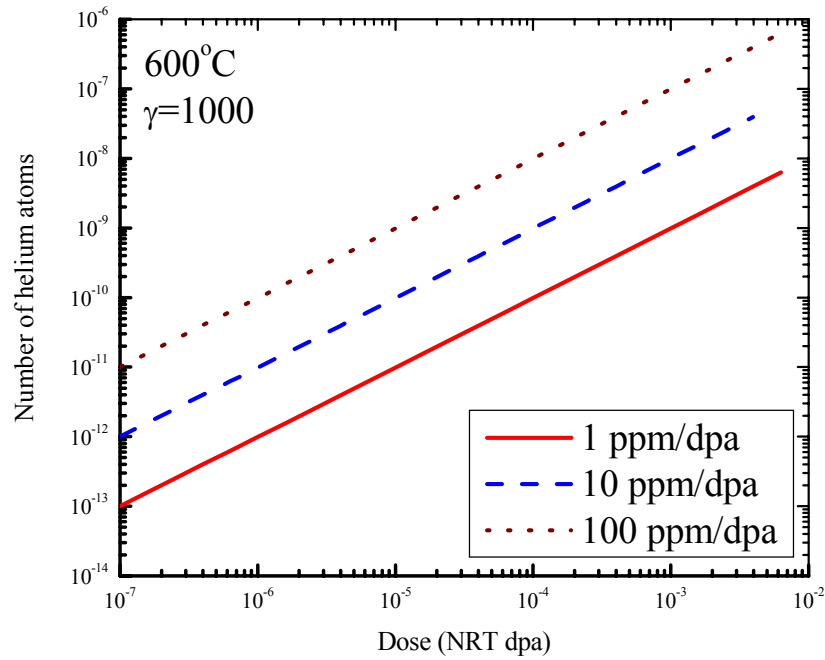


Fig. 13. Dose dependence of total number of He atoms accumulated in crystal calculated at different He generation rates under irradiation at 600°C.

It is worthy to emphasize again that the group method developed in this work provides conservation of the total number density of the clusters and the total number of point defects (vacancies and He atoms) accumulated in the clusters. An example of this can be seen in Fig. 13 where the dose dependence of the total number of He atoms

accumulated in crystal, i.e. the value $M(t) = \sum_{x=1}^{\infty} \sum_{m=1}^{\infty} mf(x, m, t) + C_{He}(t)$, is presented. As can be seen in all

cases considered the magnitude $M(t)$ is linear increased with dose increase as it has to be when He atoms are generated with constant rate.

As can be seen from Fig. 9 nucleation of the stable clusters occurs faster at higher magnitude of the He generation rate. Such a behavior takes place because it is necessary to accumulate a certain concentration of He atoms to provide the nucleation process, what requires different irradiation doses at different magnitudes of the He generation rates. Correspondingly an evolution of SDF of the clusters is quite different in the cases considered that can be seen on Figs. 14 where the SDF calculated with different He generation rates after irradiation to a dose of 10^{-3} dpa are presented. As can be seen from Fig. 14a the evolution of the clusters at the lowest rate of $G_{He}=1$ ppm/dpa is still at the nucleation stage (maximum of SDF is still located at the smallest sizes) whereas at higher rates G_{He} it already corresponds to the growth stage (Figs. 14b and 14c). Note that the variation in the number of He atoms in the clusters (the width of SDF in m -space) is less in the case of the highest generation rate, i.e. at $G_{He} = 100$ ppm/dpa.

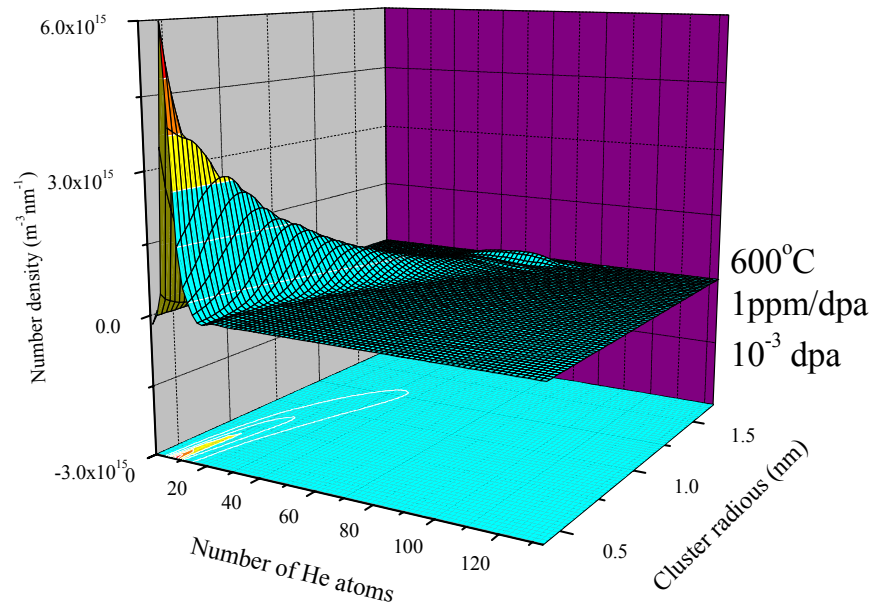


Fig. 14a. Size distribution function of the clusters at 10^{-3} dpa for the case of $G_{\text{He}} = 1 \text{ ppm} / \text{dpa}$.

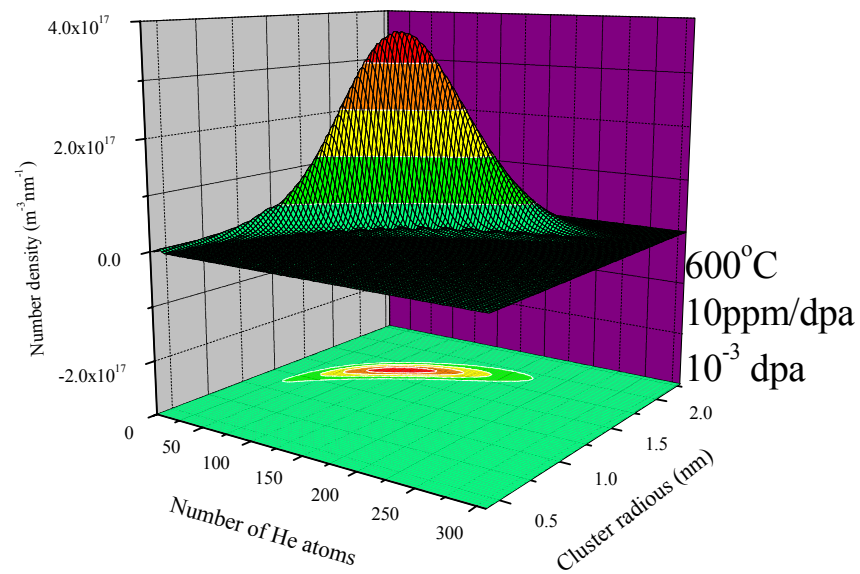


Fig. 14b. Size distribution function of the clusters at 10^{-3} dpa for the case of $G_{\text{He}} = 10 \text{ ppm} / \text{dpa}$.

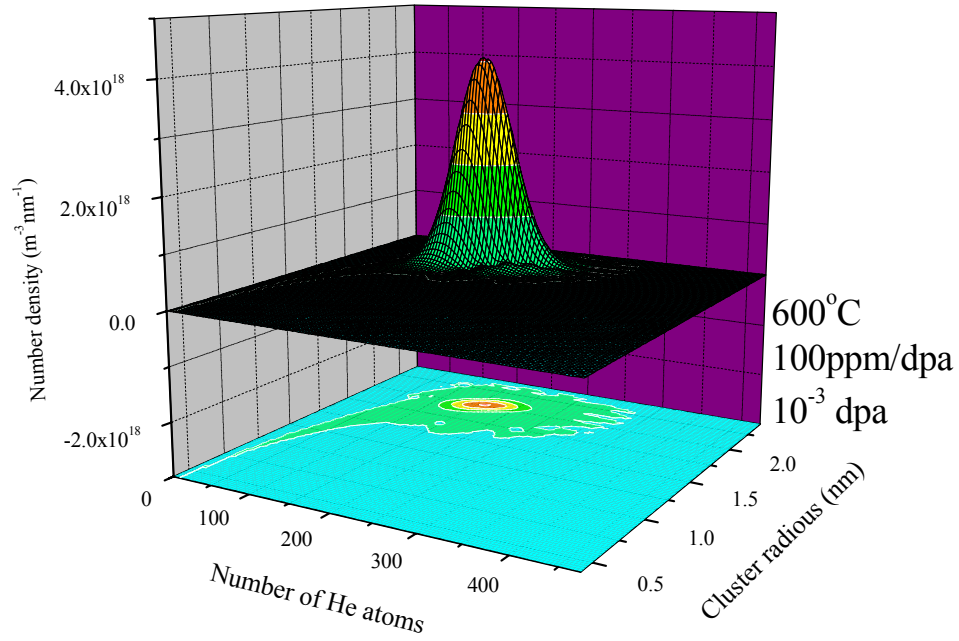


Fig. 14c. Size distribution function of the clusters at 10^{-3} dpa for the case of $G_{\text{He}} = 100 \text{ ppm/dpa}$.

The EOS effect

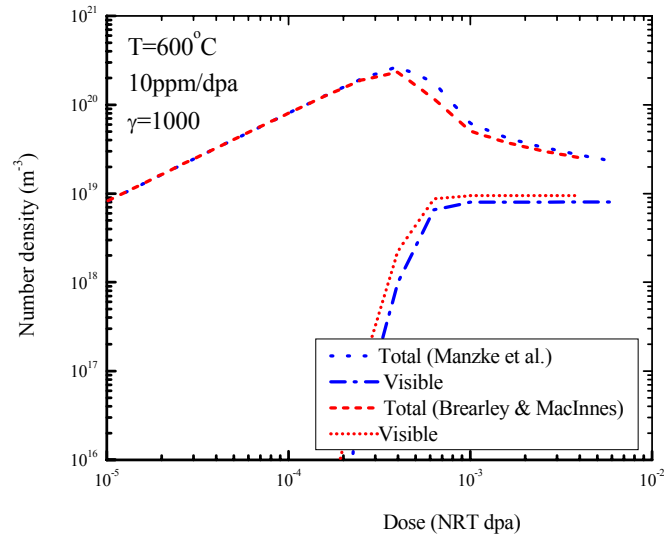


Fig. 15. Dose dependence of the cluster density calculated at 600°C and $G_{\text{He}} = 10 \text{ ppm/dpa}$ by using equation of state of He given by Eqs. (34) and (35).

All results presented above are obtained by using the equation of state of He derived by Manzke et al. (see Eq. (35)). Fig. 15 shows a comparison between the results obtained for the dose dependence of the cluster density calculated at $G_{He} = 10 \text{ ppm/dpa}$ by using the EOSs given by Eqs. (34) and (35). As can be seen the hard sphere EOS leads to a slightly higher density of the visible clusters since the hard sphere EOS provide higher stability of the clusters compare to that obtained by using the EOS described by Eq. (35). The results obtained for other values of the He generation rates are similar. Note that the total number density of the clusters obtained by using Eq. (35) is higher compare to that obtained by using the hard sphere EOS in contrast to that taking place for the visible ones.

Surface energy effect

As it has been shown above the free surface energy, γ , plays a crucial role in the case of homogeneous cluster nucleation. In order to test sensitivity of the cluster evolution to γ under irradiation with concurrent generation of He atoms the cluster evolution has been calculated for three values of γ at He generation rates to be equal 10 and 100 ppm/dpa. The results calculated are presented on Figs. 16. As can be seen at both generation rates the number density of visible clusters decreases with increasing magnitude of free surface energy however the effect is rather small. Note that similar to that found in the calculations with different EOS (see Fig. 15) the total number density of the clusters obtained in the case of the most stable clusters ($\gamma=1000$) is lower compare to that obtained in the case of when the clusters are less stable ($\gamma=1500$ and 2000).

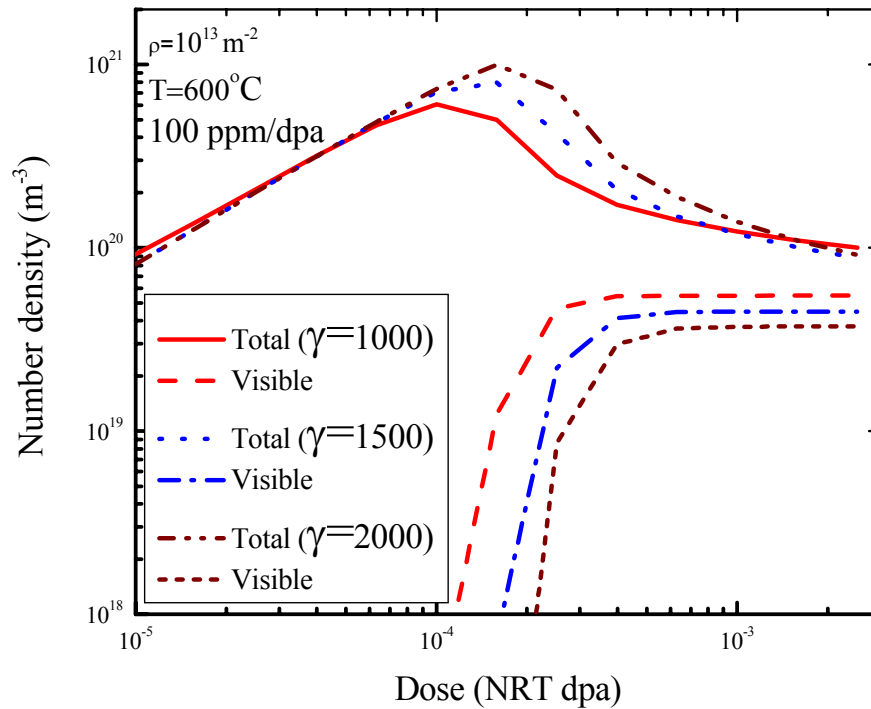


Fig. 16a. Dose dependence of the cluster density under irradiation at $G_{He} = 100 \text{ ppm/dpa}$ calculated for different values of the surface energy.

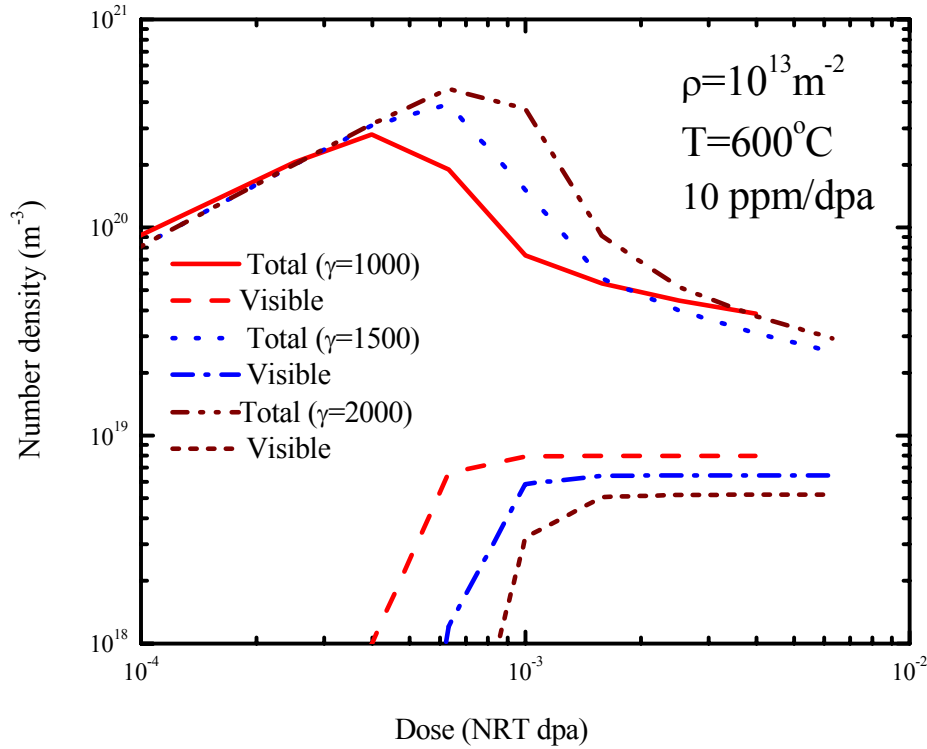


Fig. 16b. Dose dependence of the cluster density under irradiation at $G_{He} = 10 \text{ ppm/dpa}$ calculated for different values of the surface energy.

CONCLUSIONS

1. A new grouping method for an approximate solution of two dimensional kinetic equations describing evolution of point defect clusters is developed. It is shown that the method can be easily generalized to solve a kinetic equation of highest dimensionality. An ability of the method is demonstrated describing an evolution of helium–vacancy clusters under irradiation.
2. Preliminary results of the calculations of evolution of helium–vacancy clusters under irradiation are presented for a case when: (a) a concurrent generation of He atoms taking place with different rate in the range of 1-100 ppm/dpa, (b) the sink strength of defects others than the cluster is constant with dose. The results calculated are compared with those obtained in the case when there is no He generation.
3. It is found that the terminal cluster is very close to linear in the He generation rate. It is also shown that in the case of He assisted evolution of vacancy clusters: (a) nucleation of the clusters is not very sensitive to the value of surface energy in contrast to that taking place when the homogeneous nucleation operates, (b) The so called hard sphere equation of state of He [27] and that derived by Manzke et al. [28] lead to quite similar results for He-vacancy cluster evolution.

REFERENCES

1. M. Kiritani, *J. Phys. Soc. Japan* 35 (1973) 95.
2. S.I. Golubov, A.M. Ovcharenko, A.V. Barashev, and B.N. Singh, *Philos. Mag. Series A.* 81, No.3 (2001) 643-658.
3. K. Russell, *Acta Metall.* 19 (1971) 753.
4. K. Russell, *Scripta Metall.* 6 (1972) 209.
5. K. Russell, *Scripta Metall.* 7 (1973) 755.
6. K. Russell, *The theory of void nucleation in metals*, *Acta Metall.* 26 (1978) 1616.
7. S.I. Maydet and K. Russell, *Numerical simulation of void nucleation in irradiated metals*, *J. Nucl. Mater.* 82 (1979) 271.
8. J.L. Katz and H. Wiedersich, *J. Nucl. Mater.* 46 (1973) 41.
9. H. Wiedersich, J.J. Barton and J.L. Katz, *J. Nucl. Mater.* 51 (1974) 287.
10. B.T.M. Loh, *Acta Metall.* 20 (1972) 1305.
11. H. Trinkaus, *J. Nucl. Mater.* 118 (1983) 39.
12. H. Trinkaus, *J. Nucl. Mater.* 133&134 (1985) 105;
13. H. Trinkaus, *Radiation Effects*. 101 (1986) 101.
14. A.J.E. Foreman and B.N. Singh, *J. Nucl. Mater.* 141 - 143 (1986) 672.
15. H. Trinkaus, B.N. Singh and A.J.E. Foreman, *J. Nucl. Mater.* 174 (1990) 80.
16. B.N. Singh and H. Trinkaus, *J. Nucl. Mater.* 186 (1992) 153.
17. B.N. Singh and A.J.E. Foreman, *The Physics of Irradiation Produced Voids* (ed. By R.S. Nelson) HMSO, London (1975) p.205.
18. B.N. Singh and A.J.E. Foreman, *J. Nucl. Mater.* 122&123 (1992) 537.
19. A.J.E. Foreman, *Harwell Rep. AERE-R 8389*.
20. N. Ghoniem, H. Gurol, *Radiation Effects* 55 (1981) 209
21. N. Ghoniem, S. Sharafat, J.M. Williams, and L.K. Mansur, *J. Nucl. Mater.* 117 (1983) 96.
22. S. Sharafat, N. Ghoniem, *UCLA/ENG-8947* (1989) PPG-1225.
23. S. Sharafat, N. Ghoniem, *J. Nucl. Mater.* 122 (1-3) (1984) 531.
24. R.E. Stoller and G.R. Odette, *J. Nucl. Mater.* 131 (1985) 118.
25. A.M. Ovcharenko S.I. Golubov, C.H. Woo, Hanchen Huang, *GMIC++: Grouping method in C++: an efficient method to solve large number of Master equations*, *Computer Physics Communications* (in press).
26. Singh B.N., Golubov S.I., Trinkaus H., Serra A., Osetsky Yu.N., Barashev A.V., *J. Nucl. Mater.*, 251 (1997) 107-122.
27. I.R. Brearley and D.A. MacInnes, *J. Nucl. Mater.* 95 (1980) 239.
28. R. Manzke, W. Jäger, H. Trinkaus, G. Crecelius, and R. Zeller, *Solid State Communications* 44, No.4 (1982) 481.